Journal of the European Ceramic Society 23 (2003) 1167–1173

www.elsevier.com/locate/jeurceramsoc

Sintering and properties of molybdenum-doped $SrBi_2Ta_2O_9$ ceramics

Jiin-Jyh Shyu*, Chih-Chung Lee

Department of Materials Engineering, Tatung University, Taipei 104, Taiwan, ROC

Received 1 March 2002; received in revised form 13 July 2002; accepted 27 July 2002

Abstract

The effects of molybdenum doping on the sintering, microstructure, dielectric properties, and ferroelectric properties of $SrBi_2(Ta_{1-x}Mo_x)O_{9+y}$ ceramics were investigated. The densification process of the molybdenum doped ceramics with $x=0.025$–0.1 can be shifted to a lower temperature range. When the degree of densification is nearly the same, the doped ceramics showed reduced dielectric constant as compared with the undoped ceramics. For the ceramics with relative density $\geqslant 90\%$, the dielectric constant is 120–125 and 80–120 for the undoped and doped ceramics, and the dielectric loss tangent is below 2%. For nearly the same relative density, all the molybdenum-doped ceramics have significantly increased P_r and decreased E_C as compared with the undoped ceramics. There are optimum molybdenum content ($x=0.025$–0.05) and optimum sintering temperature (1100 °C) for maximum P_r and minimum E_C.

Keywords: Dielectric properties; Ferroelectric properties; Sintering; $SrBi_2Ta_2O_9$; Tantalates

1. Introduction

$SrBi_2Ta_2O_9$ (SBT) thin films have been extensively investigated as promising candidates for nonvolatile ferroelectric random access memories, because of high fatigue endurance (up to 10^{11} to 10^{12} switching cycles) and low leakage current with Pt electrodes.[1—3] However, the major disadvantages of SBT are the low remanent polarization and the high processing temperature.[4,5] It has been reported that the properties of layered perovskite SBT ferroelectrics (thin films or ceramics) can be influenced by composition modification. According to Bhattacharyya et al.,[6] the Bi content remarkably affects the ferroelectric properties of SBT thin films. Effects of Sr/Bi ratio on the phase formation, ferroelectric phase transition, dielectric properties, and ferroelectric properties have been investigated.[7—12] It has also been reported that the remanent polarization of SBT thin films can be improved by partial substitution of Sr^{2+} by Ba^{2+} [13].

$SrBi_2Ta_2O_9$ belongs to the Aurivillius family of bismuth layered perovskites of the general formula $(Bi_2O_2)^{2+}(A_{m-1}B_mO_{3m+1})^{2-}$, where $A=Na^+$, K^+, Ca^{2+}, Sr^{2+}, Ba^{2+}, Pb^{2+}, Bi^{3+}, etc., $B=Ti^{4+}$, Nb^{5+}, Ta^{5+}, Mo^{6+}, W^{6+}, Fe^{3+}, etc. and $m=1$–5.[14] In this paper, we report on the effects of molybdenum doping on the sintering, microstructure, dielectric properties, and ferroelectric properties of $SrBi_2Ta_2O_9$ in ceramic form. This study may result in materials with enhanced ferroelectric properties that are useful in applications.

2. Experimental procedure

2.1. Sample preparation

The ceramic compositions studied are $SrBi_2(Ta_{1-x}Mo_x)_2O_{9+y}$, where $x=0$, 0.025, 0.05, 0.075, 0.1, and 0.2. The ceramics were prepared by standard ceramic procedure. Reagent-grade $SrCO_3$, Bi_2O_3, Ta_2O_5, and Mo_2O_3 powders were mixed for 6 h in PE bottles containing yittria-stabilized zirconia balls and alcohol. After being dried and calcined at 900 °C for 3 h, the powders were milled for 48 h with 5.5 wt.% of polyvinyl

* Corresponding author. Tel.: +886-2-2593-6897; fax: +886-2-2593-6897.

E-mail address: jjshyu@ttu.edu.tw (J.-J. Shyu).

0955-2219/03/$ - see front matter © 2002 Elsevier Science Ltd. All rights reserved.
PII: S0955-2219(02)00276-5

alcohol as binder in PE bottles containing yittria-stabilized zirconia balls and alcohol. The slurries were then dried and screened (<100 mesh). The powders of 1.0 g were uniaxially pressed into disc compacts in a 10 mm diameter steel die lubricated with a thin layer of stearic acid. The powder compacts, which were embedded in the powder with the same composition in an alumina crucible with an alumina lid, were prefired at 550 °C for 2 h, followed by sintering at 1000–1300 °C for 3 h, and then furnace cooled.

2.2. Characterization

Phase identification was conducted by X-ray diffraction (XRD) analysis on the as-sintered surface. Measurements were performed on a diffractometer (Model D5000, Siemens, Germany) with CuK_α radiation. The operating power was 40 kV and 20 mA. Continuous scanning was used with a sampling interval of 0.02° (2θ). Bulk density (ρ_b) and open porosity for the sintered bodies were measured by the Archimedes method. The theoretical density (ρ_{th}) of $SrBi_2(Ta_{1-x}Mo_x)O_9$ was calculated by dividing the cell weight by the cell volume, which was estimated from lattice constants measured by XRD. Then, the relative density (ρ_r) of the sintered bodies was calculated by ρ_b/ρ_{th}. The as-sintered surface of the sintered bodies, coated with a thin film of gold, was examined by scanning electron microscopy (SEM).

The dielectric constant and loss tangent of the sintered bodied were measured at the room temperature by an LCR meter (Model HP4284A, Hewlett-Packard, Tokyo, Japan) with an oscillating voltage of 1 V and a frequency of 1 kHz. The sintered samples were polished to remove a thickness of about 100 μm, then were electroded by firing a 70Ag/30Pd paint at 850 °C for 30 min. For the ferroelectric loop measurement, samples were ground and polished to a thickness of 0.1– 0.2 mm, then were gold electroded by sputtering with masked edges. The *P–E* hysteresis loops were observed at room temperature using a modified Sawyer–Tower circuit with 60 Hz sinusoidal field. The samples were dipped in silicone oil during measurement.

3. Results and discussion

3.1. Densification, X-ray analysis, and microstructure

Fig. 1 shows the XRD patterns of the powders calcined at 900 °C. For the undoped composition, a single layered perovskite phase was formed. For the doped compositions, in addition to the major layered perovskite phase, a minor unknown phase was formed, especially when the molybdenum content was increased.

Fig. 2 shows the degree of densification (represented by relative density) of the sintered samples. Although

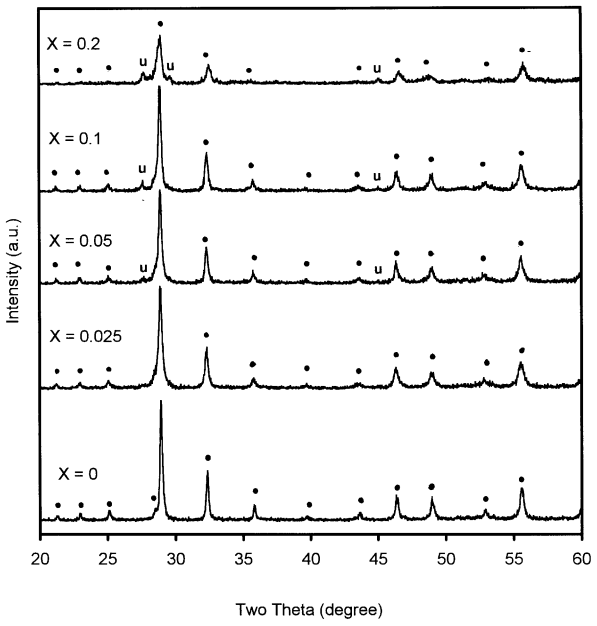

Fig. 1. XRD patterns of the as-calcined powders (●: layered perovskite, u: unknown).

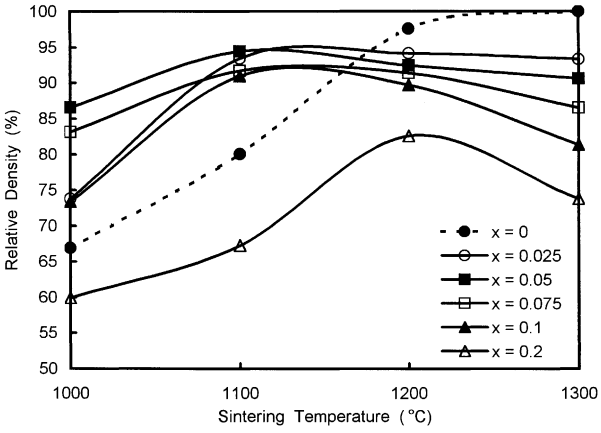

Fig. 2. Relative density of the sintered ceramics as a function of sintering temperature.

the above mentioned unknown phase was not disappeared after sintering, the theoretical density of $SrBi_2(Ta_{1-x}Mo_x)O_9$ was used as that of the ceramic because of the weak XRD intensities for the unknown phase. As seen in Fig. 2, the relative density of the undoped composition increased in the temperature range 1000–1200 °C, then approached about 97–99.9% at 1200–1300 °C. For the compositions with $x = 0.025$–0.1, the densification curve was shifted to a lower temperature range. The densification was improved when the sintering temperature was $\leqslant$1100 °C, while the densification was reduced when the sintering temperature was $\geqslant$1200 °C. The composition with $x = 0.2$ showed the lowest density at each sintering temperature. All the doped compositions, especially when x is increased, showed a density reduction at higher sintering temperatures. The

density-reduction phenomenon is consistent with the open porosity data (not shown in the paper). A relative density $\geqslant 90\%$ can be obtained for the ceramics with $x=0$ sintered at 1200–1300 °C, $x=0.025$–0.05 sintered at 1100–1300 °C, or $x=0.075$–0.1 sintered at 1100–1200 °C.

Fig. 3(a) and (b) shows the typical XRD patterns of the bodies sintered at 1000 and 1300 °C, respectively. It was found that single layered perovskite phase was formed in the undoped ceramics sintered at 1000–1300 °C. For the doped ceramics, the minor unknown phase did not disappear in addition to the major layered perovskite phase. The amount of second phase

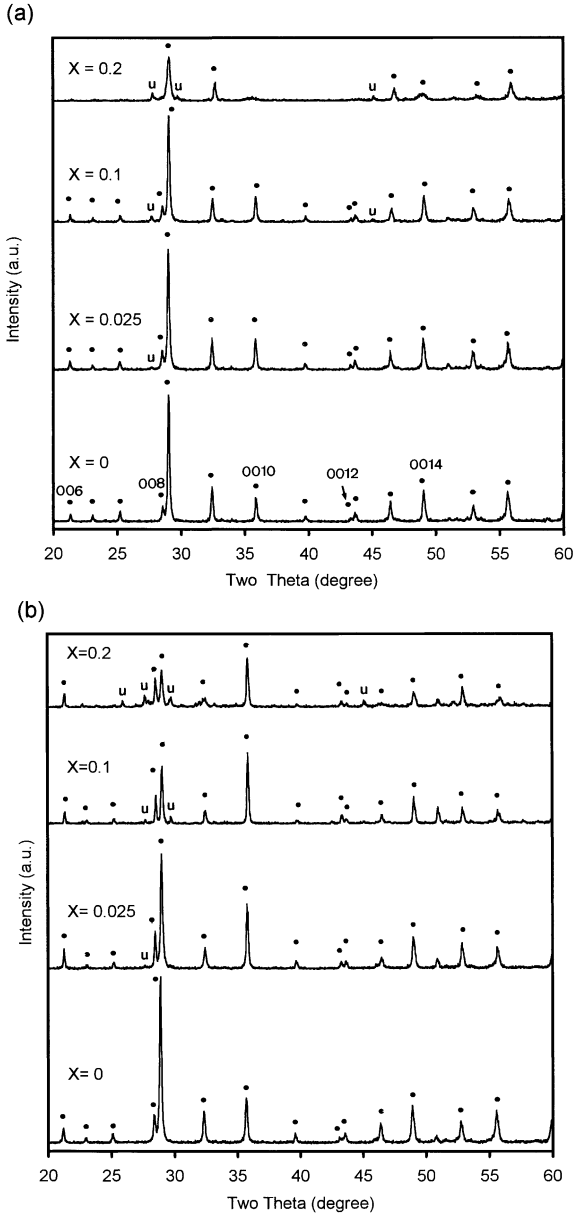

Fig. 3. Typical XRD patterns of the ceramics. The sintering temperature is (a) 1000 °C and (b) 1300 °C (●: layered perovskite, u: unknown).

increased slightly with the sintering temperature and the molybdenum content. It is also noted that the peaks of layered perovskite phase became broad and weak in the samples with $x=0.2$ (for 1000–1200 °C) or 0.1–0.2 (for 1300 °C), indicating that the crystal structure of layered perovskite became defective. This result is also observed in the calcined powder with $x=0.2$ (Fig. 1). Moreover, the doped ceramics exhibited the (00l) preferred orientation of the layered perovskite when the sintering temperature was higher [1200–1300 °C, see Fig. 3(b)). It was found that when the samples were polished to remove a thickness of about 0.4 mm, the preferred orientation vanished. It was found that the lattice constants of the layered perovskite (not shown) decreased with the increase in molybdenum content, indicating that molybdenum has been incorporated into the lattice, although a second phase is formed as seen in Fig. 3. The difference in ionic radius for Ta^{5+} (0.64 Å, CN = 6 [15]) and Mo^{n+} ion (0.67, 0.65, 0.63, and 0.60 Å for $n=3$, 4, 5, and 6, respectively, CN = 6[15]) is $<6\%$. The decreased cell volume implies that the incorporated Mo ion might have a valence of +5 or +6, because of the smaller ion sizes of Mo^{5+} or Mo^{6+} than Ta^{5+}.

Figs. 4 and 5 show the typical microstructures for the undoped and doped samples, respectively. The average grain size of the undoped samples increased smoothly when the sintering temperature was increased from 1000 to 1300 °C. At temperatures $\leqslant 1100$ °C [Fig. 4(a)], the microstructure consists of nearly equiaxed grains, although a few grains show anisotropic shape. The grain size is about 0.5–1 μm at 1100 °C. When the sintering temperature was increased to 1200–1300 °C (Fig. 4(b) and (c)], most of the grains reveal anisotropic shape with aspect ratios of about 2.5–4 at 1300 °C. For all the doped samples, the temperature at which the grain shape becomes anisotropic reduced to 1100 °C [see Fig. 5(a) for $x=0.025$]. When the sintering temperature is increased to 1200 °C, almost all the grains are plate-like [see Fig. 5(b) for $x=0.025$]. The microstructure became coarser at 1300 °C, as seen in Fig. 5(c). Moreover, the average grain-size and the aspect ratio of the plate-like grains increased abruptly. It is also noted that the average grain-size and the aspect ratio of the plate-like grains at 1200–1300 °C increased with the increase in molybdenum content.

The above described microstructure development might explain the density result shown in Fig. 2. The density reduction at 1200–1300 °C for each doped composition should be caused by the abrupt increase in grain-size and the fully developed plate-like-grained microstructure. The densification process is usually inhibited by rapid grain growth. Moreover, the plate-like grains with a high aspect ratio, when impinge each other, might also suppress the densification process due to the large growth-rate anisotropy. Evidence supporting this hypothesis is that the undoped composition

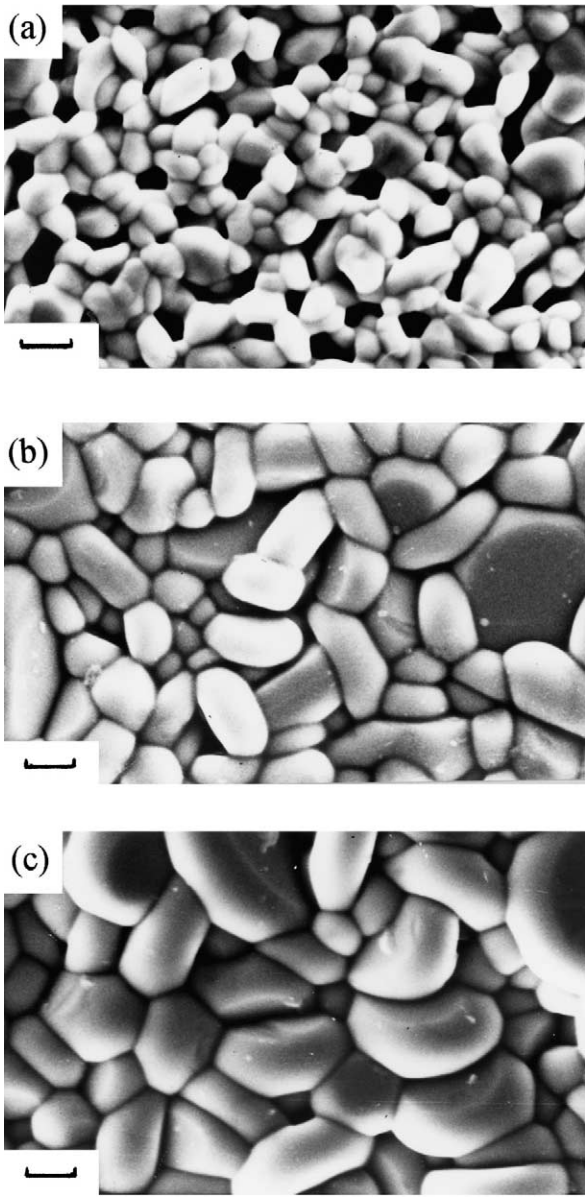

Fig. 4. Microstructures of the ceramics with $x=0$ sintered at (a) 1100 °C, (b) 1200 °C, and (c) 1300 °C (bar = 1 μm).

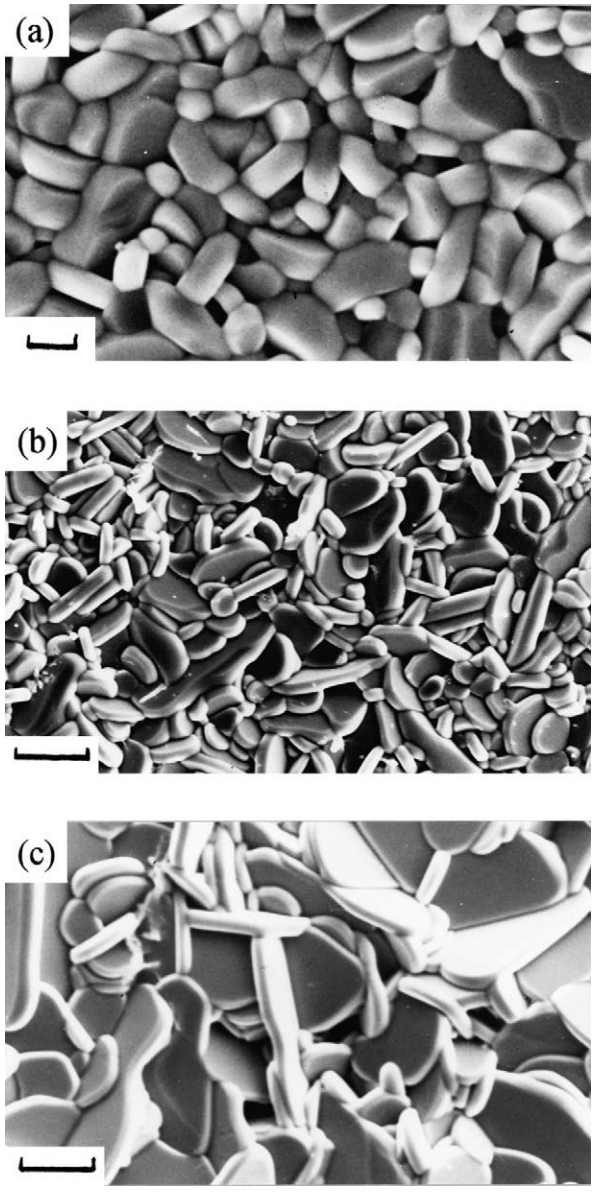

Fig. 5. Microstructures of the doped ceramics with $x=0.025$ sintered at (a) 1100 °C (bar = 1 μm), (b) 1200 °C, and (c) 1300 °C (bar = 5 μm).

does not show density reduction because no abrupt increase in grain size occurs and the plate-like-grained microstructure is not fully developed.

3.2. Dielectric properties and ferroelectric properties

The dielectric constant (κ') at 1 kHz as a function of sintering temperature is shown in Fig. 6(a). The κ'-value of the undoped composition first increased from 90 to 125 in the temperature range 1000–1200 °C, mainly due to the increase in relative density from 67 to 97%, followed by a slight decrease in κ' to 120 at 1300 °C, although the density is higher than the ceramic sintered at 1200 °C. For the doped compositions, κ' was more reduced at 1200–1300 °C. Moreover, when the sintering temperature is in the range of 1000–1100 °C, the κ'-value first increased with x, then decreased. While when the sintering temperature is in the range of 1200–1300 °C, the κ'-value decreased with x. For the doped ceramics with relative density $\geqslant 90\%$, the κ'-value is in the range of 80–120. The above trends of κ' for both undoped and doped ceramics are quite similar with those of densification (Fig. 2), indicating that densification has a large effect on κ'. Fig. 6(b) shows the dependence of κ' on relative density. The curves link the data points in accordance with the sequence of sintering temperature (the data points for 1300 °C are indicated by the arrows). It is obvious for each composition that the increase in relative density does not promise higher κ'-value. This result indicates that, in addition to sintered density, there

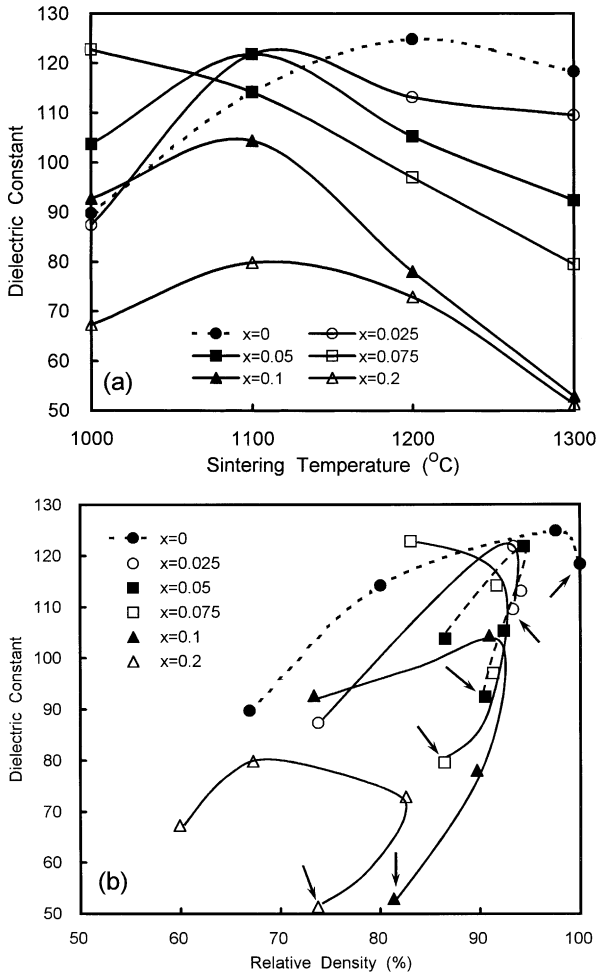

Fig. 6. Dielectric constant at 1 kHz as a function of (a) sintering temperature and (b) relative density.

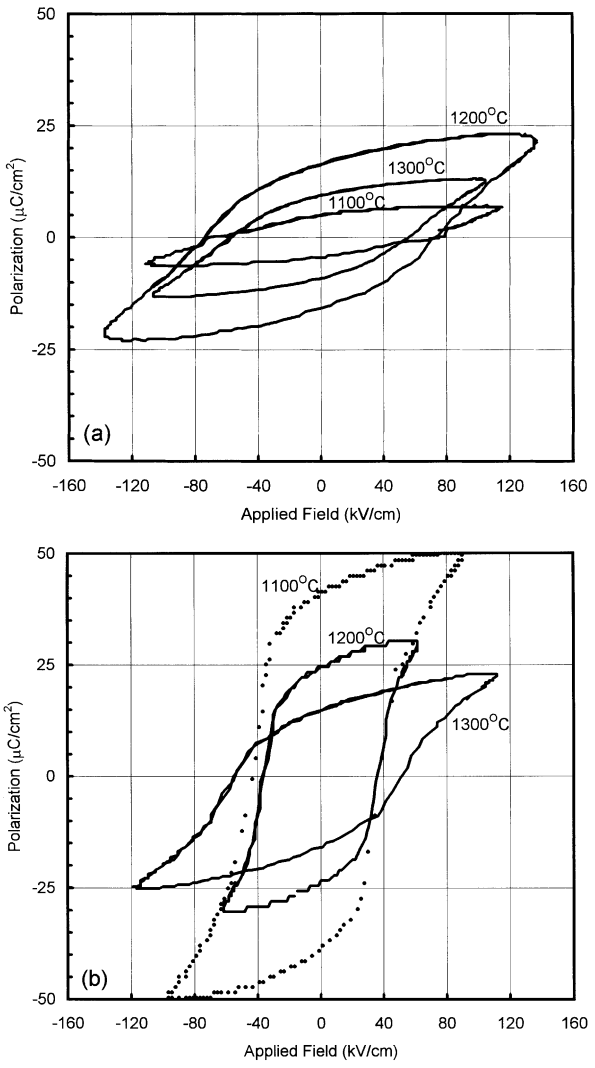

Fig. 7. *P–E* hysteresis loops of the ceramics with x=(a) 0 and (b) 0.025 sintered at 1100–1300 °C.

are other factors influencing the dielectric constant. Moreover, when relative density is nearly the same the doped samples showed reduced κ' as compared with the undoped samples. This result suggested that doping of molybdenum will reduce the dielectric constant if the effect of densification can be eliminated. The dielectric constant might also be affected by other factors. The decrease in κ' at higher molybdenum content and higher sintering temperature might be caused by the slight increase in the content of phase U (Fig. 3), the more defective structure of the layered perovskite phase (Fig. 3, when x is 0.1–0.2), preferred orientation (Fig. 3, at higher sintering temperature), and/or the increased grain-size (Fig. 5). The dielectric loss tangent (tanδ) for the samples with relative density $\geqslant$90% is below 2%.

Fig. 7(a) shows the typical *P–E* hysteresis loops for the undoped ceramics. The loop is slim and non-saturated until the sintering temperature is $\geqslant$1200 °C. The P_r- and E_C-values decreased from 16 μC/cm² and 72 kV/cm for 1200 °C to 8.9 μC/cm² and 60 kV/cm for 1300 °C, possibly caused by the coarse microstructure [Fig. 4(c)]. However, saturated loops can be observed for the ceramics with x=0.025–0.1 sintered at 1000°–1300 °C, as shown typically in Fig. 7(b) for x=0.025, except for x=0.025 at 1000 °C. The loops for x=0.2 became saturated when the sintering temperature is $\geqslant$1200 °C. The loops are non-saturated mainly due to poor densification.

The values of P_r and E_c for the ceramics with a saturated loop (except for x=0 at 1000 and 1100 °C) are shown in Fig. 8(a) and (b), respectively. It is obvious that addition of molybdenum significantly increased P_r (except for x=0.2) and decreased E_C. For the same sintering temperature, it is generally that P_r first increased with x then decreased, and E_C first decreased with x then increased. The optimum molybdenum content (x) for maximum P_r and minimum E_C is 0.025–0.05. It is also noted that, for the same molybdenum content, there is an optimum sintering temperature for maximum P_r (1100 °C for x=0.025–0.1 and 1200 °C for x=0 and 0.2). While the E_C-value increased (for x=0

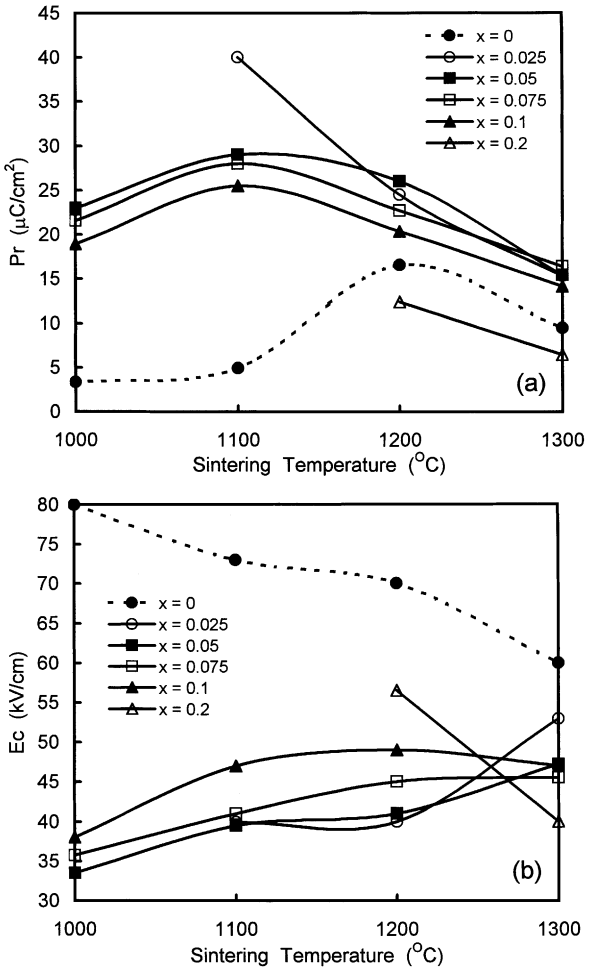

Fig. 8. (a) P_r and (b) E_C as a function of sintering temperature.

and 0.2) or decreased (for $x = 0.025$–0.1) with the increase in sintering temperature.

To cancel out the porosity effect, figures similar to Fig. 6(b) have been plotted (not shown). It is found that for nearly the same relative density, all the doped samples have increased P_r and decreased E_C as compared with the undoped samples. It has been reported that partial substitution of Nb^{5+} in $SrBi_2Nb_2O_9$ ceramic by a smaller cation V^{5+} can improve the ferroelectric properties,[16] due to the enlarged rattling space. In the present study, the smaller ionic size of Mo^{6+} might have the similar effect. The decrease in P_r at higher molybdenum content and higher sintering temperature might be caused by the density reduction (Fig. 2) due to the rapid coarsening in microstructure, slight increase in the amount of second phase (Fig. 3), and/or the more defective structure of the layered perovskite phase (Fig. 3, when x is 0.1–0.2).

4. Conclusions

The effects of molybdenum doping on the densification, microstructure, and properties of $SrBi_2(Ta_{1-x}Mo_x)O_{9+y}$ ceramics were investigated, with the following results:

1. Single layered perovskite phase was formed in the undoped ceramics. For the doped ceramics, a minor unknown phase was formed in addition to the major layered perovskite phase.
2. The densification process of the molybdenum doped ceramics with $x = 0.025$–0.1 can be shifted to a lower temperature range. All the doped compositions showed a density reduction at higher sintering temperature, possibly caused by the abrupt increase in grain size and the fully developed plate-like-grained microstructure.
3. When the degree of densification is nearly the same, the doped ceramics showed reduced dielectric constant as compared with the undoped ceramics. For the ceramics with relative density $\geqslant 90\%$, the dielectric constant is 120–125 and 80–120 for the undoped and doped ceramics, and the dielectric loss tangent is below 2%.
4. For nearly the same relative density, all the molybdenum-doped ceramics have significantly increased P_r and decreased E_C as compared with the undoped ceramics. There are optimum molybdenum content ($x = 0.025$–0.05) and optimum sintering temperature (1100 °C) for maximum P_r and minimum E_C.

References

1. Paz de Araujo, C. A., Cuchiaro, J. D., McMillan, L. D., Scott, M. C. and Scott, J. F., Fatigue-free ferroelectric capacitors with platinum electrodes. *Nature (London)*, 1995, **374**, 627–629.
2. Desu, S. B. and Li, T., Fatigue-free $SrBi_2(Ta_xNb_{2-x})O_9$ ferroelectric thin films. *Mater. Sci. Eng.*, 1995, **B34**, L4–L8.
3. Desu, S. B. and Vijay, D. P., c-Axis oriented ferroelectric $SrBi_2(Ta_xNb_{2-x})O_9$ thin films. *Mater. Sci. Eng.*, 1995, **B32**, 83–88.
4. Scott, J. F., Layer perovskite thin films and memory devices. In *Thin Film Ferroelectric Materials and Devices*, ed. R. Ramech. Kluwer, Norwell, MA, 1997, pp. 115.
5. Scott, J. F., High dielectric constant thin films for dynamic random access memories (DRAM). *Ann. Rev. Mater. Sci.*, 1998, **28**, 79–100.
6. Bhattacharyya, S., James, A. R. and Krupanidhi, S. B., Role of growth conditions and Bi-content on the properties of $SrBi_2Ta_2O_9$ thin films. *Solid State Comm.*, 1998, **108**, 759–763.
7. Noguchi, T., Hase, T. and Miyasaki, Y., *Jpn. J. Appl. Phys.*, 1996, **35**, 4900.
8. Kojima, S. and Saitoh, I., Soft phonon and bismuth content in ferroelectric $SrBi_2Ta_2O_9$. *Physic B*, 1999, **263–264**, 653–656.
9. Torii, Y., Tato, K., Tsuzuki, A., Hwang, H. J. and Dey, S. K., Preparation and dielectric properties of nonstoichiometric $SrBi_2Ta_2O_9$ based ceramics. *J. Mater. Sci. Lett.*, 1998, **17**, 827–828.
10. Miura, M. and Tanaka, M., Jpn. *J. Appl. Phys.*, 1998, **37**, 2554.
11. Watanabe, H., Mihara, T., Yoshimori, H. and Araujo, C. A. P., *Jpn J. Appl. Phys.*, 1995, **34**, 5240.
12. Rodriguez, M. A., Boyle, T. J., Hernandez, B. A., Buchheit, C. D.

and Eatough, M. O., Formation of $SrBi_2Ta_2O_9$: part II evidence of a bismuth-deficient pyrochlore phase. *J. Mater. Res.*, 1996, **11**, 2282–2287.

13. Lu, C. and Wen, C., Preparation and properties of barium incorporated strontium bismuth tantalate ferroelectric thin films. *Mater. Res. Soc. Symp. Proc.*, 1999, **541**, 229–234.
14. Aurivillius, B., Mixed bismuth oxides with layer lattices. *Ark. Kemi*, 1949, **1**, 463–470.
15. Shannon, R. D. and Prewitt, C. T., Effective ionic radii in oxides and fluorides. *Acta. Crystallogr.*, 1969, **B25**, 925–945.
16. Wu, Y. and Cao, G., Influences of vanadium doping on ferroelectric properties of strontium bismuth niobates. *J. Mater. Sci. Lett.*, 2000, **19**, 267–269.